Reverse Micellar Organization and Dynamics: A Wavelength-Selective Fluorescence Approach

Amitabha Chattopadhyay,* Soumi Mukherjee, and H. Raghuraman

Centre for Cellular & Molecular Biology, Uppal Road, Hyderabad 500 007, India

Received: August 1, 2002; In Final Form: September 30, 2002

Wavelength-selective fluorescence comprises a set of approaches based on the red edge effect in fluorescence spectroscopy, which can be used to directly monitor the environment and dynamics around a fluorophore in a complex biological system. A shift in the wavelength of maximum fluorescence emission toward higher wavelengths, caused by a shift in the excitation wavelength toward the red edge of the absorption band, is termed the red edge excitation shift (REES). This effect is mostly observed with polar fluorophores in motionally restricted media such as very viscous solutions or condensed phases. We have previously shown that REES and related techniques (wavelength-selective fluorescence approach) offer a novel way to monitor organization and dynamics of membrane- and micelle-bound probes and peptides. In this paper, we report REES of NBD-PE, a phospholipid whose headgroup is covalently labeled with the 7-nitrobenz-2-oxa-1,3-diazol-4-yl (NBD) moiety, when incorporated into reverse micelles formed by sodium bis(2-ethylhexyl) sulfosuccinate (AOT) in heptane with varying amounts of added water. Fluorescence parameters such as intensity, emission maximum, and REES of NBD-PE incorporated in AOT reverse micelles were found to be dependent on the [water]/[surfactant] molar ratio (w_o). Interestingly, the extent of REES was found to decrease with increasing w_o. Time-resolved fluorescence measurements of NBD-PE in AOT/heptane reverse micelles show a significant reduction in the mean fluorescence lifetime with increasing w_o. In addition, fluorescence polarization and mean fluorescence lifetime of NBD-PE in reverse micellar environments were found to be wavelength-dependent. Taken together, these results are indicative of the motional restriction experienced by the fluorophore when bound to reverse micelles and its modulation with the [water]/[surfactant] molar ratio. Wavelength-selective fluorescence promises to be a powerful tool for exploring reverse micellar organization and dynamics under various conditions.

Introduction

Amphiphilic surfactants self-assemble to form reverse (or inverted) micelles in nonpolar solvents in which the polar headgroups of the surfactant monomers cluster to form a micellar core and are directed toward the center of the assembly and the hydrophobic tails extend outward into the bulk organic phase.[1,2] Reverse micelles can solubilize an appreciable amount of water to form a spherical pool in the center. They are optically transparent nanometer-sized water droplets of various size surrounded by a layer of surfactant molecules dispersed in nonpolar solvents. The studies on reverse micellar organization and dynamics assume special significance in light of the fact that the general principles underlying their formation are common to other related assemblies such as micelles, bilayers, liposomes, and biological membranes.[3−6] The double chain anionic surfactant AOT (sodium bis(2-ethylhexyl) sulfosuccinate) has been extensively used to form reverse micelles in nonpolar solvents. For reviews on AOT, see refs 7 and 8. One of the main reasons for using AOT is that reverse micelles formed by AOT can solubilize a large quantity of water in a nonpolar solvent.

The water pools entrapped in reverse micelles have been extensively used as micromedia for chemical and biochemical reactions. The nature of water in reverse micelles, especially at low water content, has been studied extensively and is believed to be different from that of bulk water. The highly structured yet heterogeneous water molecules in reverse micelles represent interesting models for water molecules present in biological systems such as membranes, which are more difficult to analyze experimentally. The physical and chemical properties of the entrapped water are markedly different from the properties of bulk water but similar in several aspects to those of biological interfacial water as found in membrane or protein interfaces.[9−12] The interfacial water plays a crucial role in the induction of secondary structure in peptides and proteins when bound to surfaces such as membranes as well as for variation of their local internal motion. Both experimental[9−12] and theoretical[13] approaches have shown that the key structural parameter of reverse micelles is the [water]/[surfactant] molar ratio (w_o), which determines their size as well as the extent of deviation of the properties of the entrapped water from those of normal bulk water. Reverse micelles thus represent a type of organized molecular assembly that offers the unique advantage of monitoring dynamics of molecules with varying degrees of hydration. A wide range of physicochemical properties of the micellar water including micropolarity, dielectric constant, microviscosity, water activity, freezing point, proton transfer efficiency, and the hydrogen-bonding potential of the aqueous inner core can be experimentally varied with w_o therefore providing a unique and versatile reaction medium.

Fluorescence techniques have been widely used to characterize reverse micellar organization and dynamics due to suitable time scale, noninvasive nature, and intrinsic sensitivity.[14]

* To whom correspondence should be addressed. Tel: +91-40-2719-2578. Fax: +91-40-2716-0311. E-mail: amit@ccmb.res.in.

10.1021/jp021801m CCC: $22.00 © 2002 American Chemical Society
Published on Web 11/19/2002

Reverse micelles offer certain inherent advantages in fluorescence studies since they are small and optically transparent, have well-defined sizes, and are relatively scatter-free. They are highly cooperative, organized molecular assemblies of amphiphilic surfactants and are dynamic in nature. A direct consequence of such organized systems is the restriction imposed on the dynamics and mobility of their constituent structural units. We have previously shown that the microenvironment of molecules bound to such organized assemblies can be conveniently monitored using wavelength-selective fluorescence as a novel tool.[15−24] Wavelength-selective fluorescence comprises a set of approaches based on the red edge effect in fluorescence spectroscopy, which can be used to directly monitor the environment and dynamics around a fluorophore in a complex biological system.[25−28] A shift in the wavelength of maximum fluorescence emission toward higher wavelengths, caused by a shift in the excitation wavelength toward the red edge of absorption band, is termed red edge excitation shift (REES). This effect is mostly observed with polar fluorophores in motionally restricted media such as very viscous solutions or condensed phases where the dipolar relaxation time for the solvent shell around a fluorophore is comparable to or longer than its fluorescence lifetime.[25−31] REES arises from slow rates of solvent relaxation (reorientation) around an excited state fluorophore (as compared to the fluorescence lifetime), which is a function of the motional restriction imposed on the solvent molecules in the immediate vicinity of the fluorophore. Utilizing this approach, it becomes possible to probe the mobility parameters of the environment itself (which is represented by the relaxing solvent molecules) using the fluorophore merely as a reporter group. Furthermore, because the ubiquitous solvent for biological systems is water, the information obtained in such cases will come from the otherwise "optically silent" water molecules. The unique feature about REES is that while all other fluorescence techniques (such as fluorescence quenching, energy transfer, and polarization measurements) yield information about the fluorophore (either intrinsic or extrinsic) itself, REES provides information about the relative rates of solvent (water in biological systems) relaxation dynamics, which is not possible to obtain by other techniques. This makes the use of REES in particular and the wavelength-selective fluorescence approach in general extremely useful since hydration plays a crucial modulatory role in a large number of important cellular events such as protein folding, lipid−protein interactions, and ion transport.[32−37]

We have previously shown that REES and related techniques (wavelength-selective fluorescence approach) serve as a powerful tool to monitor organization and dynamics of probes and peptides bound to membranes[15−18,20−22,24] and membrane-mimetic media such as micelles.[19,23] In addition, we have previously used the wavelength-selective fluorescence approach to analyze the organization and dynamics of tryptophans in the soluble hemolytic protein α-toxin[21] and the cytoskeletal protein tubulin, which is a component of the microtubular network in eukaryotes.[38]

In this paper, we report the observation of red edge excitation effects of N-(7-nitrobenz-2-oxa-1,3-diazol-4-yl)-1,2-dipalmitoyl-*sn*-glycero-3-phosphoethanolamine (NBD-PE) when incorporated into reverse micelles formed by AOT in heptane. NBD-labeled lipids are widely used as fluorescent analogues of native lipids in biological and model membranes to study a variety of processes.[39,40] In NBD-PE, the NBD group is covalently attached to the headgroup of a phosphatidylethanolamine molecule. The NBD group in NBD-PE has earlier been shown to be localized in the interfacial region of the membrane,[41−46] and its location in the reverse micellar environment is most likely to be interfacial. Reverse micelles represent a type of organized molecular assembly, which offers the unique advantage of monitoring dynamics of molecules with varying states of hydration. Application of the wavelength-selective fluorescence approach to reverse micellar systems is therefore particularly appealing since REES is capable of monitoring the dynamics of the solvent molecules surrounding the fluorophore.

Experimental Section

Materials. AOT was purchased from Sigma Chemical Co. (St. Louis, MO). NBD-PE was obtained from Molecular Probes (Eugene, OR). Water was purified through a Millipore (Bedford, MA) Milli-Q system and used throughout. The heptane used was of spectroscopic grade. The purity of AOT was confirmed by good agreement of its UV absorption spectrum with previously reported spectrum.[1] The purity of NBD-PE was checked by thin-layer chromatography on silica gel precoated plates (Sigma) in chloroform/methanol/water (65:35:5, v/v/v) and was found pure when detected by its color or fluorescence. Concentrations of stock solutions of NBD-PE in methanol were estimated using their molar absorption coefficient (ϵ) of 21 000 M^{-1} cm^{-1} at 463 nm.[24]

Preparation of Reverse Micelles. Reverse micelles of AOT-containing NBD-PE were prepared without addition of any cosolvent as follows. NBD-PE in methanol (12 nmol) was dried under a stream of nitrogen while being warmed gently (∼35 °C). After it was further dried under a high vacuum for at least 4 h, 1.5 mL of 50 mM AOT in heptane was added and samples were vortexed for 3 min. The samples were kept in the dark for an hour with intermittent vortexing (10 s of vortexing at intervals of 10 min) to incorporate the fluorescent probe NBD-PE into the reverse micelles and to obtain optically clear dispersions. Appropriate amounts of water were subsequently added to make reverse micellar dispersions of different [water]/[surfactant] molar ratio (w_o). The optical density of the fluorescent samples at the excitation wavelength was low (generally <0.18) in all cases. Background samples were prepared the same way except that NBD-PE was not added to them. All experiments were done at room temperature (23 °C).

The molar ratio of fluorophore to surfactant was carefully chosen to give an optimum signal-to-noise ratio with minimal perturbation to the micellar organization and negligible interprobe interactions. The final fluorophore (NBD-PE) concentration in the reverse micelles was 8 μM while the concentration of AOT was 50 mM in all cases. This corresponds to a final molar ratio of fluorophore to surfactant of 1:6250 (mol/mol). At such a low fluorophore to surfactant molar ratio, not more than one probe molecule would be present per reverse micelle on an average, which rules out any probe aggregation effects, especially keeping in mind the aggregation number of AOT of ∼50−183 in the range of w_o between 5 and 20.[47]

Steady State Fluorescence Measurements. Steady state fluorescence measurements were performed with a Hitachi F-4010 spectrofluorometer using 1 cm path length quartz cuvettes. Excitation and emission slits with a nominal bandpass of 3 nm were used for all measurements. Background intensities of samples in which the fluorophore NBD-PE was omitted were negligible in most cases and were subtracted from each sample spectrum to cancel out any contribution due to the solvent Raman peak and other scattering artifacts. Fluorescence polarization measurements were performed using a Hitachi

polarization accessory. Polarization values were calculated from the equation[48]

$$P = \frac{I_{VV} - GI_{VH}}{I_{VV} + GI_{VH}} \quad (1)$$

where I_{VV} and I_{VH} are the measured fluorescence intensities (after appropriate background subtraction) with the excitation polarizer vertically oriented and emission polarizer vertically and horizontally oriented, respectively. G is the grating correction factor and is equal to I_{HV}/I_{HH}. All experiments were done with multiple sets of samples, and average values of polarization are shown in the figures. The spectral shifts obtained with different sets of samples were identical in most cases. In other cases, the values were within ±1 nm of the ones reported.

Time-Resolved Fluorescence Measurements. Fluorescence lifetimes were calculated from time-resolved fluorescence intensity decays using a Photon Technology International (London, Western Ontario, Canada) LS-100 luminescence spectrophotometer in the time-correlated single photon counting mode. This machine uses a thyratron-gated nanosecond flash lamp filled with nitrogen as the plasma gas (16 ± 1 in of mercury vacuum) and is run at 22−25 kHz. Lamp profiles were measured at the excitation wavelength using Ludox (colloidal silica) as the scatterer. To optimize the signal-to-noise ratio, 10 000 photon counts were collected in the peak channel. All experiments were performed using excitation and emission slits with a nominal band-pass of 4 nm or less. The sample and the scatterer were alternated after every 5% acquisition to ensure compensation for shape and timing drifts occurring during the period of data collection. This arrangement also prevents any prolonged exposure of the sample to the excitation beam thereby avoiding any possible photodamage of the fluorophore. Nevertheless, we recorded the fluorescence emission spectra of the fluorophore before and after the time-resolved data acquisition, and the spectra remained unchanged indicating no photodamage during data acquisition. This is an important control since NBD-labeled lipids have previously been reported to be photobleached under certain conditions.[39] The data stored in a multichannel analyzer was routinely transferred to an IBM PC for analysis. Intensity decay curves so obtained were fitted as a sum of exponential terms:

$$F(t) = \sum_i \alpha_i \exp(-t/\tau_i) \quad (2)$$

where α_i is a preexponential factor representing the fractional contribution to the time-resolved decay of the component with a lifetime τ_i. The decay parameters were recovered using a nonlinear least squares iterative fitting procedure based on the Marquardt algorithm.[49] The program also includes statistical and plotting subroutine packages.[50] The goodness of the fit of a given set of observed data and the chosen function were evaluated by the reduced χ^2 ratio, the weighted residuals,[51] and the autocorrelation function of the weighted residuals.[52] A fit was considered acceptable when plots of the weighted residuals and the autocorrelation function showed random deviation about zero with a minimum χ^2 value not more than 1.5. Mean (average) lifetimes $\langle\tau\rangle$ for biexponential decays of fluorescence were calculated from the decay times and preexponential factors using the following equation[53]

$$\langle\tau\rangle = \frac{\alpha_1\tau_1^2 + \alpha_2\tau_2^2}{\alpha_1\tau_1 + \alpha_2\tau_2} \quad (3)$$

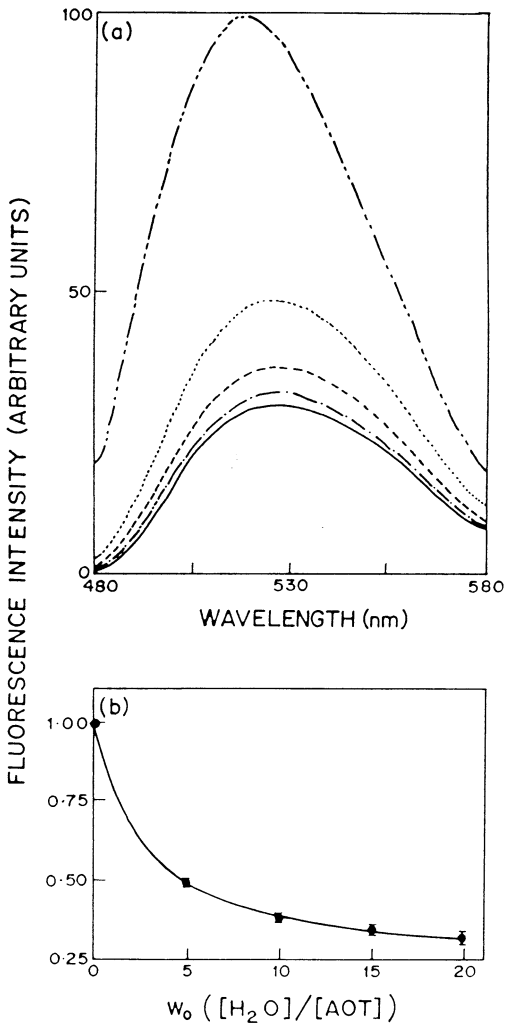

Figure 1. Effect of increasing amounts of added water on (a) fluorescence emission spectra and (b) fluorescence intensity of NBD-PE in reverse micelles of AOT in heptane. Fluorescence emission spectra in (a) are shown as a function of [water]/[surfactant] molar ratio (w_o) in order of decreasing intensity corresponding to w_o = 0 (— - -), 5 (- - -), 10 (— —), 15 (· — ·), and 20 (—). Fluorescence intensity was monitored at 521 nm and is plotted as a function of w_o in (b). The data points shown are the means of three independent measurements. The error bars represent the standard error. The excitation wavelength used was 465 nm, and the ratio of fluorophore (NBD-PE) to surfactant (AOT) was 1:6250 (mol/mol) in all cases. See Experimental Section for other details.

Results

We have earlier reported that the fluorescence emission maxima of NBD-PE incorporated in model membranes of dioleoyl-*sn*-glycero-3-phosphocholine (DOPC)[15] and in sodium dodecyl sulfate (SDS) micelles[19] are ~531 nm. The fluorescence emission spectra of NBD-PE in reverse micelles of AOT in heptane as a function of increasing [water]/[surfactant] molar ratio (w_o) are shown in Figure 1a. In contrast to the emission maximum of NBD-PE in membranes and micelles, the maximum of fluorescence emission of NBD-PE in AOT/heptane reverse micelles without any added water (w_o = 0) is found to be at 515 nm. This blue shift in emission maximum indicates the nonpolar nature of the site of localization of the NBD group in the reverse micellar assembly. However, after the water content is increased, i.e., when w_o is increased from 0 to 20, the emission maximum displays a progressive red shift of 13 nm from 515 to 528 nm (see Table 1). The quantum yield of NBD fluorescence is known to depend on the polarity of the

TABLE 1: Fluorescence Emission Maxima of NBD-PE in AOT/Heptane Reverse Micelles as a Function of w_o

[water]/[surfactant] molar ratio[a] (w_o)	emission maximum[b] (nm)
0	515
5	525
10	526
15	527
20	528

[a] The ratio of NBD-PE to AOT was 1:6250 (mol/mol). [b] The excitation wavelength used was 465 nm.

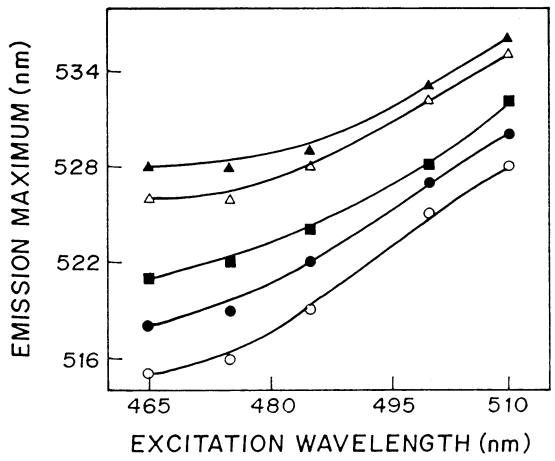

Figure 2. Effect of changing excitation wavelength on the wavelength of maximum emission of NBD-PE in reverse micelles of AOT in heptane corresponding to $w_o = 0$ (○), 1 (●), 2 (■), 10 (△), and 20 (▲). All other conditions are as in Figure 1. See Experimental Section for other details.

medium in which the probe is located and is reduced in polar environments.[54,55] Figure 1a shows that the red shift in emission maximum of NBD-PE is accompanied with ~70% reduction in peak fluorescence intensity when w_o is increased from 0 to 20. We attribute this decrease in fluorescence to an increase in the polarity around the NBD group due to an increase in water content. The decrease in fluorescence intensity of NBD-PE at 521 nm as a function of increasing w_o is shown in Figure 1b.

The shifts in the maxima of fluorescence emission[56] of NBD-PE when bound to reverse micelles of AOT/heptane as a function of excitation wavelength are shown in Figure 2. As the excitation wavelength is changed from 465 to 510 nm, the emission maxima of NBD-PE bound to reverse micelles of varying w_o display shifts toward longer wavelengths in all cases. The emission maxima are shifted from 515 to 528 nm (in the case of reverse micelles with no added water, i.e., $w_o = 0$), 518 to 530 nm ($w_o = 1$), 521 to 532 nm ($w_o = 2$), 526 to 535 nm ($w_o = 10$), and 528 to 536 nm ($w_o = 20$), which correspond to REES of 8−13 nm in these cases. Such dependence of the emission spectra on the excitation wavelength is characteristic of the red edge effect. Observation of this effect in reverse micelles implies that the NBD group of NBD-PE, when incorporated in these micelles, is in an environment where its mobility is considerably reduced. Because the NBD group is believed to be localized in the interfacial region, such a result would directly imply that this region of the reverse micelle offers considerable restriction to the reorientational motion of the solvent dipoles around the excited state fluorophore. The interfacial region of reverse micelles is associated with bound water with characteristic dynamics.[9−13] These results therefore assume significance in the context of recent reports of slow (~nanoseconds) water relaxation in reverse micelles.[57−59]

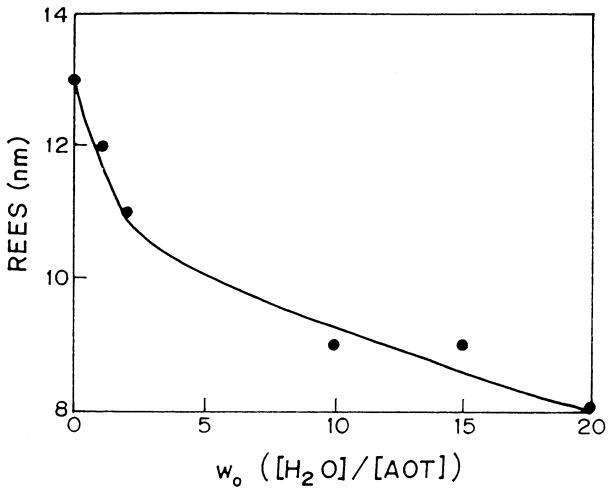

Figure 3. Effect of increasing amounts of water on the magnitude of REES of NBD-PE in reverse micelles of AOT in heptane. REES data obtained from Figure 2 are plotted as a function of [water]/[surfactant] molar ratio (w_o). All other conditions are as in Figure 1. See Experimental Section for other details.

TABLE 2: Lifetimes of NBD-PE in AOT/Heptane Reverse Micelles as a Function of w_o[a]

[water]/[surfactant] molar ratio[b] (w_o)	α_1	τ_1 (ns)	α_2	τ_2 (ns)	χ^2
0	0.75	11.92	0.25	6.04	1.08
5	0.78	8.16	0.22	3.32	1.00
10	0.80	6.77	0.20	3.39	1.25
15	0.76	5.15	0.24	6.91	1.12
20	0.72	5.69	0.28	3.73	1.06
25	0.87	5.37	0.13	2.86	1.13
30	0.81	5.22	0.19	2.80	1.12

[a] The excitation wavelength was 465 nm; emission was monitored at 521 nm. [b] The ratio of NBD-PE to AOT was 1:6250 (mol/mol).

The magnitude of REES obtained from Figure 2 as a function of w_o is shown in Figure 3. As is apparent from the figure, the extent of REES is found to decrease with increasing water to surfactant ratio indicating that the overall motional restriction experienced by the reorienting solvent molecules is reduced as more water is added to the reverse micelles. Similar results have previously been obtained with an amphiphilic hemicyanine dye.[60] This essentially means that there is a reorganization of the water molecules in the reverse micellar assembly upon increasing the water to surfactant molar ratio (w_o) from 0 to 20. This is in excellent agreement with earlier reports in which it was shown that water relaxation rates in reverse micelles become faster with an increase in w_o.[58]

The phenomenon of REES is based on differential extents of solvent reorientation around the excited state fluorophore, with each excitation wavelength selectively exciting a different average population of fluorophores.[24−27] Because fluorescence lifetime serves as a sensitive indicator for the local environment in which a given fluorophore is placed and is known to be sensitive to excited state interactions, differential extents of solvent relaxation around a given fluorophore could be expected to give rise to differences in its lifetime. Table 2 shows the lifetimes of NBD-PE in AOT/heptane reverse micelles as a function of w_o. All fluorescence decays for reverse micelle-bound NBD-PE obtained as a function of w_o could be fitted well with biexponential function.

The mean fluorescence lifetimes of NBD-PE bound to AOT/heptane reverse micelles were calculated from Table 2 using eq 3 and are plotted as a function of increasing w_o in Figure 4.

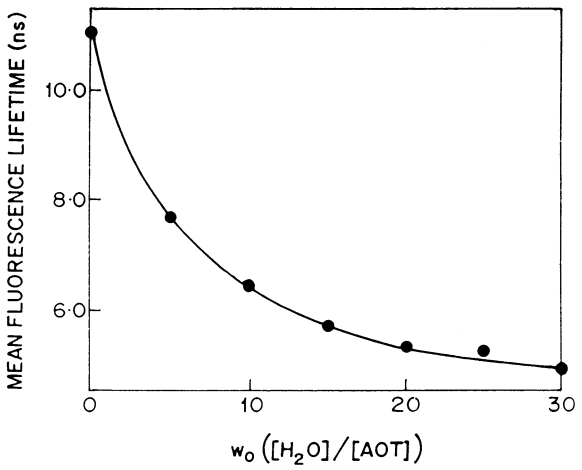

Figure 4. Effect of increasing amounts of water on mean fluorescence lifetime of NBD-PE in AOT/heptane reverse micelles. Samples were excited at 465 nm while emission was monitored at 521 nm. Mean fluorescence lifetimes were calculated from Table 2 using eq 3. All other conditions are as in Figure 1. See Experimental Section for other details.

We chose to use the mean fluorescence lifetime as an important parameter for describing the behavior of NBD-PE bound to AOT/heptane reverse micelles since it is independent of the method of analysis and the number of exponentials used to fit the time-resolved fluorescence decay. There is a continuous decrease in mean lifetime of NBD-PE with increased water content in the micelle. Thus, the mean lifetime decreases from ~11 to ~5 ns (i.e., by more than 50%) when the [water]/[surfactant] molar ratio (w_o) is changed from 0 to 30. This is consistent with previous observations in which it was reported that NBD lifetime reduces in the presence of water.[54,55,61] In pure water, NBD lifetime reduces to ~1.5 ns, which has been attributed to hydrogen-bonding interactions between the fluorophore and the solvent,[54] which is accompanied by an increase in the rate of nonradiative decay.[40,61]

Table 3 shows the lifetimes of NBD-PE in reverse micelles of AOT/heptane as a function of excitation wavelength, keeping the emission wavelength constant at 521 nm. All fluorescence decays could be fitted well with a biexponential function. The mean fluorescence lifetimes were calculated using eq 3 and are plotted as a function of excitation wavelength in Figure 5. As shown in this figure, there is a decrease in the mean lifetimes of NBD-PE (especially toward longer wavelengths) with increasing excitation wavelength from 465 to 505 nm when incorporated in reverse micelles of a range of [water]/[surfactant] molar ratio (w_o). Such a marked shortening of mean fluorescence lifetimes at the red edge of the absorption band is indicative of slow solvent reorientation around the excited state fluorophore.[15,17,25]

Figure 6 shows the lifetimes of NBD-PE bound to AOT/heptane reverse micelles as a function of emission wavelength, keeping the excitation wavelength constant at 465 nm. All decays corresponding to different emission wavelengths could be fitted to monoexponential functions. As can be seen from the figure, the lifetime shows a considerable increase with increasing emission wavelength from 515 to 555 nm in all cases. Figure 6 also shows that the increase in mean lifetimes is more pronounced at lower w_o values where the water pool is more structured.[12] Similar observations of increasing lifetime with increasing emission wavelength have previously been reported for fluorophores in environments of restricted mobility.[15,17,25] Such increasing lifetimes across the emission spectrum may be

TABLE 3: Lifetimes of NBD-PE as a Function of Excitation Wavelength[a]

excitation wavelength (nm)	α_1	τ_1 (ns)	α_2	τ_2 (ns)	χ^2
		(a) $w_o = 5$			
465	0.78	8.16	0.22	3.32	1.00
475	0.80	8.31	0.20	5.23	1.05
485	0.82	8.20	0.18	2.92	1.01
495	0.88	7.84	0.12	1.59	1.14
505	0.58	1.08	0.42	7.53	1.19
		(b) $w_o = 10$			
465	0.80	6.77	0.20	3.39	1.25
475	0.90	6.70	0.10	2.85	1.08
485	0.66	7.05	0.34	5.11	1.16
495	0.74	5.29	0.26	7.67	1.16
505	0.78	0.82	0.22	6.20	1.19
		(c) $w_o = 15$			
465	0.76	5.15	0.24	6.91	1.12
475	0.90	6.20	0.10	2.57	1.28
485	0.81	6.16	0.19	1.41	1.00
495	0.80	5.99	0.20	2.32	1.16
505	0.77	1.03	0.23	5.84	1.34
		(d) $w_o = 20$			
465	0.72	5.69	0.28	3.73	1.06
475	0.74	5.45	0.26	4.58	1.07
485	0.67	5.48	0.33	4.79	1.05
495	0.52	5.17	0.48	0.60	1.25
505	0.60	0.60	0.40	4.54	1.22

[a] Emission wavelength 521 nm.

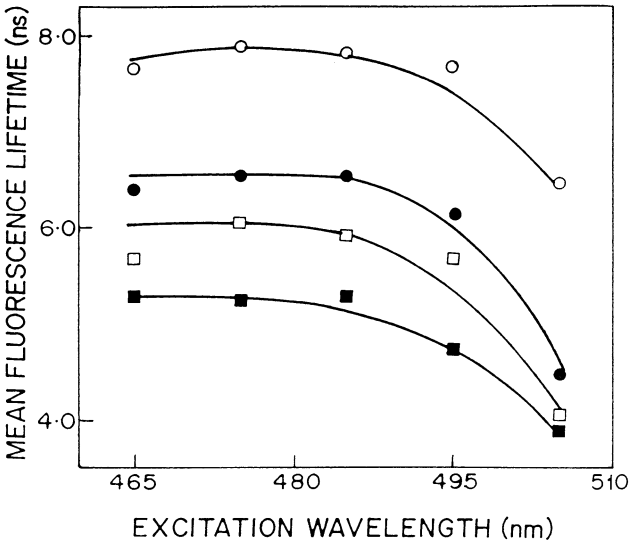

Figure 5. Mean fluorescence lifetime of NBD-PE in AOT/heptane reverse micelles as a function of excitation wavelength. Emission wavelength was kept constant at 521 nm. Mean lifetimes were calculated from Table 3 using eq 3. Data shown correspond to reverse micelles with w_o = 5 (○), 10 (●), 15 (□), and 20 (■). All other conditions are as in Figure 1. See Experimental Section for other details.

interpreted in terms of solvent reorientation around the excited state fluorophore as follows. Observation at shorter wavelengths of emission spectra selects for predominantly unrelaxed fluorophores. Their lifetimes are shorter because this population is decaying both at the rate of fluorescence emission at the given excitation wavelength and by decay to longer (unobserved) wavelengths. In contrast, observation at the long wavelength (red edge) of the emission selects for the more relaxed fluorophores, which have spent enough time in the excited state to allow increasingly larger extents of solvent relaxations.

These longer-lived fluorophores, which emit at higher wavelengths, should have more time to rotate in the excited

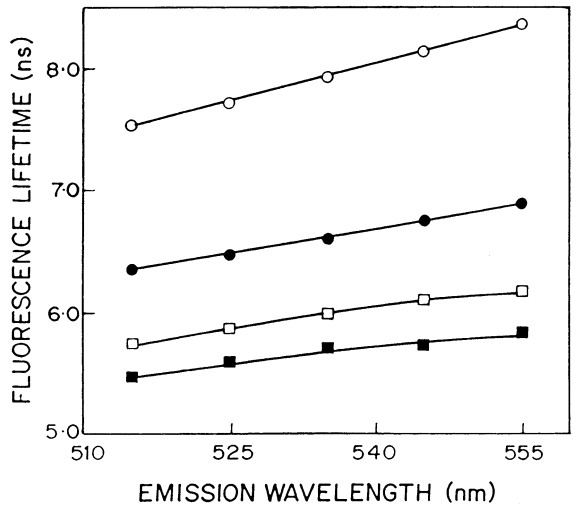

Figure 6. Fluorescence lifetime of NBD-PE in AOT/heptane reverse micelles as a function of emission wavelength. Excitation wavelength used was 465 nm. Data shown correspond to reverse micelles with $w_o = 5$ (○), 10 (●), 15 (□), and 20 (■). All other conditions are as in Figure 1. See Experimental Section for other details.

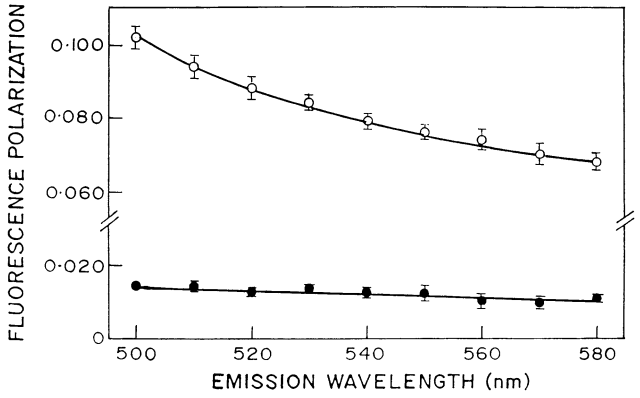

Figure 7. Fluorescence polarization of NBD-PE in AOT/heptane reverse micelles corresponding to $w_o = 15$ (○) and in methanol (●) as a function of emission wavelength. The concentration of NBD-PE in methanol was 8 μM. The excitation wavelength was 465 nm in all cases. The data points shown are the means of three independent measurements. The error bars represent the standard error. All other conditions are as in Figure 1. See Experimental Section for other details.

state, giving rise to lower polarization. Figure 7 shows representative data showing the variation in the steady state polarization of NBD-PE in AOT/heptane reverse micelles corresponding to $w_o = 15$ as a function of wavelength across its emission spectrum. As seen in the figure, there is a considerable decrease in polarization with increasing emission wavelength. The lowest polarization is observed toward longer wavelengths (red edge) where emission from the relaxed fluorophores predominates. Similar observations have previously been reported for other fluorophores in environments of restricted mobility.[25] In a control experiment, the variation in the steady state polarization of NBD-PE in methanol was monitored as a function of emission wavelength and was found to be essentially invariant (see Figure 7). This gives further support to our interpretation of the wavelength-selective fluorescence effects for NBD-PE incorporated into reverse micelles.

Discussion

Reverse micelles are relatively simple yet versatile systems and represent ideal systems to address a variety of problems in biology including their application as reaction media[62] and in protein biotechnology.[63] They represent an attractive model system for biomembranes since they mimic a number of important and essential features of biological membranes although lacking much of the complexity associated with biological membranes. Reverse micelles offer the unique advantage of monitoring dynamics of bound molecules with varying degrees of hydration by varying the [water]/[surfactant] molar ratio (w_o), which is difficult to achieve with complex systems such as membranes.

Wavelength-selective fluorescence has been previously applied for monitoring protein dynamics and conformation in solution[25,27,31] as well as in more complex systems such as the intact eye lens.[64,65] We have earlier applied this approach for studying organization and dynamics of membrane- and micelle-bound probes and peptides.[15−24] Application of the wavelength-selective fluorescence approach to reverse micellar organization and dynamics has been the focus of this paper. We show here that NBD-PE, when incorporated into reverse micelles of AOT with varying amounts of water content, exhibits wavelength-selective fluorescence effects. Our results show that fluorescence parameters such as intensity, emission maximum, and REES of NBD-PE incorporated in AOT reverse micelles depend on the [water]/[surfactant] molar ratio (w_o). More importantly, the extent of REES was found to decrease with increasing w_o indicating that REES is sensitive to changing hydration and it is possible to detect differences in water dynamics that is accompanied with increasing water content. Time-resolved fluorescence measurements of NBD-PE in AOT/heptane reverse micelles show a significant reduction in the mean fluorescence lifetime with increasing w_o. In addition, fluorescence polarization and mean fluorescence lifetime of NBD-PE in reverse micellar environments were found to be wavelength-dependent. Taken together, these results imply motional restriction experienced by the fluorophore when bound to reverse micelles and its modulation with the [water]/[surfactant] molar ratio. This implies that the NBD group of NBD-PE, when bound to AOT reverse micelles, is in a motionally restricted environment. Furthermore, because the NBD group is most likely to be localized in the interfacial region, our results show that this region of the micelle offers considerable restriction to the reorientational motion of the solvent dipoles around the excited state fluorophore.

The choice of a suitable probe is of considerable importance in wavelength-selective fluorescence studies of organized molecular assemblies.[15] The probe chosen for this work (NBD-PE) is appropriate since the location of the NBD group in NBD-PE is expected to be interfacial, a region in the reverse micellar organization that is important from structural and functional aspects and is characterized by unique dynamics of water molecules. More importantly, we have earlier shown using solvatochromic and quantum chemical approaches that the dipole moment of the NBD group changes by ~4 D upon excitation,[66] an important criterion for a fluorophore to exhibit REES effects.[25] Furthermore, the NBD group possesses some of the most desirable properties for serving as an excellent probe for both spectroscopic as well as microscopic applications.[67,68] It is very weakly fluorescent in water, and after it is transferred to hydrophobic media, it fluoresces brightly in the visible range and shows a large degree of environmental sensitivity.[42,54,55,66,69] This large degree of environmental sensitivity of NBD fluorescence can prove to be very useful in probing different types of reverse micellar organizations formed under various conditions of the [water]/[surfactant] molar ratio. For example, the observation that NBD lifetimes are known to be shortened in

the presence of water[54,55,61] could prove to be an effective tool in exploring water dynamics in reverse micelles with varying degress of the [water]/[surfactant] molar ratio.

It is known that the dynamics of liquids in confined spaces is different than that of their bulk counterparts,[12,70] and this constitutes one of the main reasons for the popularity that reverse micelles enjoy as a model system in studies of water dynamics. The highly structured yet heterogeneous water molecules in reverse micelles represent interesting models for water molecules present in biological systems such as membranes, which are more difficult to analyze experimentally. Moreover, the dimension, shape, and overall charge of reverse micelles can be conveniently modulated, which makes them particularly useful for monitoring the dynamics of confined liquids. The properties of water in reverse micelles of AOT at low w_o values are rather different from those of bulk water.[9−12] Even at higher water content ($w_o = 50$), the apparent microviscosity is 6−9 times greater than that of free aqueous solutions.[71] Three types of water populations (pools) have been shown to coexist in reverse micelles. These are bound water, trapped water, and free water.[10,11,57] The crucial parameter is the [water]/[surfactant] molar ratio, which determines the relative proportions of these three types of water pools. Our results show that wavelength-selective fluorescence in general, and REES in particular, is sensitive to the changing dynamic hydration profile (see Figure 3) and can be conveniently used to probe dynamics of molecules in various states of hydration.

The ability of a fluorophore incorporated in a reverse micellar assembly to exhibit red edge effects will depend on a number of factors such as its polarity, as well as the effective polarity of its immediate environment and its fluorescence characteristics (e.g., lifetime). Because all of these properties of a probe are a function of its location in the reverse micelle, the extent of REES could very well be dependent on its location in the reverse micelle. Furthermore, reverse micelles can be of any desired charge type and can adopt different shapes and internal packing, depending on the chemical structures of the constituent monomers.[9] Whether such changes in reverse micellar organizations can be detected using the wavelength-selective fluorescence approach poses an interesting possibility. We conclude that wavelength-selective fluorescence promises to be a powerful approach for monitoring micellar organization and dynamics including conformation and dynamics of peptides and proteins incorporated into such assemblies.

Acknowledgment. We thank Y. S. S. V. Prasad and G. G. Kingi for technical help. This work was supported by the Council of Scientific and Industrial Research, Government of India. We thank members of our laboratory for critically reading the manuscript. S.M. thanks the Council of Scientific & Industrial Research for the award of a Junior Research Fellowship. H.R. was awarded a Senior Research Fellowship by the University Grants Commission.

References and Notes

(1) Luisi, P. L.; Magid, L. J. *CRC Crit. Rev. Biochem.* **1986**, *20*, 409.
(2) Luisi, P. L.; Giomini, M.; Pileni, M. P.; Robinson, B. H. *Biochim. Biophys. Acta* **1988**, *947*, 209.
(3) Tanford, C. *Science* **1978**, *200*, 1012.
(4) Israelachvili, J. N.; Marcelja, S.; Horn, R. G. *Q. Rev. Biophys.* **1980**, *13*, 121.
(5) Tanford, C. *The Hydrophobic Effect: Formation of Micelles and Biological Membranes*; Wiley-Interscience: New York, 1980.
(6) Tanford, C. *Biochem. Soc. Trans.* **1987**, *15*, 1S.
(7) De, T. K.; Maitra, A. *Adv. Colloid Interface Sci.* **1995**, *59*, 95.
(8) Moulik, S. P.; Mukherjee, K. *Proc. Indian Natl. Acad. Sci*. **1996**, *62*, 215.
(9) Venables, D. S.; Huang, K.; Schmuttenmaer, C. A. *J. Phys. Chem. B* **2001**, *105*, 9132.
(10) Ikushima, Y.; Saito, N.; Arai, M. *J. Colloid Interface Sci.* **1997**, *186*, 254.
(11) Jain, T. K.; Varshney, M.; Maitra, A. *J. Phys. Chem.* **1989**, *93*, 7409.
(12) Brubach, J.-B.; Mermet, A.; Filabozzi, A.; Gerschel, A.; Lairez, D.; Krafft, M. P.; Roy, P. *J. Phys. Chem. B* **2001**, *105*, 430.
(13) Faeder, J.; Ladanyi, B. M. *J. Phys. Chem. B* **2000**, *104*, 1033.
(14) Behera, G. B.; Mishra, B. K.; Behera, P. K.; Panda, M. *Adv. Colloid Interface Sci.* **1999**, *82*, 1.
(15) Chattopadhyay, A.; Mukherjee, S. *Biochemistry* **1993**, *32*, 3804.
(16) Chattopadhyay, A.; Rukmini, R. *FEBS Lett.* **1993**, *35*, 341.
(17) Mukherjee, S.; Chattopadhyay, A. *Biochemistry* **1994**, *33*, 5089.
(18) Chattopadhyay, A.; Mukherjee, S.; Rukmini, R.; Rawat, S. S.; Sudha, S. *Biophys. J.* **1997**, *73*, 839.
(19) Rawat, S. S.; Mukherjee, S.; Chattopadhyay, A. *J. Phys. Chem. B* **1997**, *101*, 1922.
(20) Ghosh, A. K.; Rukmini, R.; Chattopadhyay, A. *Biochemistry* **1997**, *36*, 14291.
(21) Raja, S. M.; Rawat, S.; Chattopadhyay, A.; Lala, A. K. *Biophys. J.* **1999**, *76*, 1469.
(22) Chattopadhyay, A.; Mukherjee, S. *Langmuir* **1999**, *15*, 2142.
(23) Rawat, S. S.; Chattopadhyay, A. *J. Fluoresc.* **1999**, *9*, 233.
(24) Chattopadhyay, A.; Mukherjee, S. *J. Phys. Chem. B* **1999**, *103*, 8180.
(25) Mukherjee, S.; Chattopadhyay, A. *J. Fluoresc.* **1995**, *5*, 237 and references therein.
(26) Chattopadhyay, A. In *Fluorescence Spectroscopy, Imaging and Probes*; Kraayenhof, R., Visser, A. J. W. G., Gerritsen, H. C., Wolfbeis, O., Eds.; Springer-Verlag: Heidelberg, 2002; pp 211−224.
(27) Demchenko, A. P. *Luminescence* **2002**, *17*, 19.
(28) Chattopadhyay, A. *Chem. Phys. Lipids*, in press.
(29) Galley, W. C.; Purkey, R. M. *Proc. Natl. Acad. Sci. U.S.A.* **1970**, *67*, 1116.
(30) Lakowicz, J. R.; Keating-Nakamoto, S. *Biochemistry* **1984**, *23*, 3013.
(31) Demchenko, A. P. *Trends Biochem. Sci.* **1988**, *13*, 374.
(32) Ho, C.; Stubbs, C. D. *Biophys. J.* **1992**, *63*, 897.
(33) Kandori, H.; Yamazaki, Y.; Sasaki, J.; Needleman, R.; Lanyi, J. K.; Maeda, A. *J. Am. Chem. Soc.* **1995**, *117*, 2118.
(34) Sankararamakrishnan, R.; Sansom, M. S. P. *FEBS Lett.* **1995**, *377*, 377.
(35) Haussinger, D. *Biochem. J.* **1996**, *313*, 697.
(36) Nishimura, S.; Kandori, H.; Maeda, A. *Photochem. Photobiol.* **1997**, *66*, 796.
(37) Halbhuber, K.-J., Ed. *Cell. Mol. Biol.* **2001**, *47* (5).
(38) Guha, S.; Rawat, S. S.; Chattopadhyay, A.; Bhattacharyya, B. *Biochemistry* **1996**, *35*, 13426.
(39) Chattopadhyay, A. *Chem. Phys. Lipids* **1990**, *53*, 1.
(40) Mazeres, S.; Schram, V.; Tocanne, J.-F.; Lopez, A. *Biophys. J.* **1996**, *71*, 327.
(41) Chattopadhyay, A.; London, E. *Biochemistry* **1987**, *26*, 39.
(42) Chattopadhyay, A.; London, E. *Biochim. Biophys. Acta* **1988**, *938*, 24.
(43) Pagano, R. E.; Martin, O. C. *Biochemistry* **1988**, *27*, 4439.
(44) Mitra, B.; Hammes, G. G. *Biochemistry* **1990**, *29*, 9879.
(45) Wolf, D. E.; Winiski, A. P.; Ting, A. E.; Bocian, K. M.; Pagano, R. E. *Biochemistry* **1992**, *31*, 2865.
(46) Abrams, F. S.; London, E. *Biochemistry* **1993**, *32*, 10826.
(47) Zhou, G.-W.; Li, G.-Z.; Chen, W. J. *Langmuir* **2002**, *18*, 4566.
(48) Chen, R. F.; Bowman, R. L. *Science* **1965**, *147*, 729.
(49) Bevington, P. R. *Data Reduction and Error Analysis for the Physical Sciences*; McGraw-Hill: New York, 1969.
(50) O'Connor, D. V.; Phillips, D. *Time-Correlated Single Photon Counting*; Academic Press: London, 1984; pp 180−189.
(51) Lampert, R. A.; Chewter, L. A.; Phillips, D.; O'Connor, D. V.; Roberts, A. J.; Meech, S. R. *Anal. Chem.* **1983**, *55*, 68.
(52) Grinvald, A.; Steinberg, I. Z. *Anal. Biochem.* **1974**, *59*, 583.
(53) Lakowicz, J. R. *Principles of Fluorescence Spectroscopy*; Kluwer-Plenum: New York, 1999.
(54) Lin, S.; Struve, W. S. *Photochem. Photobiol.* **1991**, *54*, 361.
(55) Fery-Forgues, S.; Fayet, J. P.; Lopez, A. *J. Photochem. Photobiol. A* **1993**, *70*, 229.
(56) We have used the term maximum of fluorescence emission in a somewhat wider sense here. In every case, we have monitored the wavelength corresponding to maximum fluorescence intensity, as well as the center of mass of the fluorescence emission. In most cases, both of these methods yielded the same wavelength. In cases where minor discrepancies were found, the center of mass of emission has been reported as the fluorescence maximum.
(57) Hazra, P.; Sarkar, N. *Chem. Phys. Lett.* **2001**, *342*, 303.

(58) Sarkar, N.; Das, K.; Datta, A.; Das, S.; Bhattacharyya, K. *J. Phys. Chem.* **1996**, *100*, 10523.
(59) Bhattacharyya, K.; Bagchi, B. *J. Phys. Chem. A* **2000**, *104*, 10603.
(60) Hof, M.; Lianos, P.; Laschewsky, A. *Langmuir* **1997**, *13*, 2181.
(61) Saha, S.; Samanta, A. *J. Phys. Chem. B* **1998**, *102*, 7903.
(62) Carvalho, C. M. L.; Cabral, J. M. S. *Biochimie* **2000**, *82*, 1063.
(63) Melo, E. P.; Aires-Barros, M. R.; Cabral, J. M. S. *Biotech. Annu. Rev.* **2001**, *7*, 87.
(64) Rao, S. C.; Rao, Ch. M. *FEBS Lett*. **1994**, *337*, 269.
(65) Rao, Ch. M.; Rao, S. C.; Rao, P. B. *Photochem. Photobiol*. **1989**, *50*, 399.
(66) Mukherjee, S.; Chattopadhyay, A.; Samanta, A.; Soujanya, T. *J. Phys. Chem.* **1994**, *98*, 2809.
(67) Mukherjee, S.; Chattopadhyay, A. *Biochemistry* **1996**, *35*, 1311.
(68) Rukmini, R.; Rawat, S. S.; Biswas, S. C.; Chattopadhyay, A. *Biophys. J.* **2001**, *81*, 2122.
(69) Rajarathnam, K.; Hochman, J.; Schindler, M.; Ferguson-Miller, S. *Biochemistry* **1989**, *28*, 3168.
(70) Granick, S. *Science* **1991**, *253*, 1374.
(71) Andrade, S. M.; Costa, S. M. B.; Pansu, R. *Photochem. Photobiol.* **2000**, *71*, 405.